Kernel Dependence of Autocorrelation Times Measured by the Master-Field Technique in Field-Transformation HMC

S. Yamamoto[1] P. A. Boyle[1] T. Izubuchi[1] L. Jin[2] C. Lehner[3]
N. Matsumoto[4]

[1]Brookhaven National Laboratory

[2]Department of Physics
University of Connecticut

[3]University of Regensburg

[4]Department of Physics
University of Boston

Lattice 2026

Table of Contents

Table of Contents

Field-Transformation HMC

With $U = \mathcal{F}_t(V)$,

$$Z = \int \mathcal{D}U e^{-S(U)} = \int \mathcal{D}V \mathrm{Det}[\mathcal{F}_*(V)]\, e^{-S(\mathcal{F}(V))} = \int \mathcal{D}V\, e^{-S_{FT}(V)}$$

$$S_{FT} = S(\mathcal{F}_t(V)) - \mathrm{ln\ Det}\mathcal{F}_*(V).$$

- inspired by flowed HMC, originally proposed by Luscher [Lüscher, 2010]
- perfect trivialization: $S_{FT} = 0$

In our study,

- approximate the trivializing map by the Wilson flow
- discretize the transformation with step of size ρ
- The number of integration steps of the discretized trivializing map is restricted to at most two

Previous Findings

FTHMC with a single stout-like smearing step on 32^4 with $\beta = 2.37$ and $2+1$ DWF at $m_\pi = 371(5)$ MeV
[Yamamoto et al., 2025, Blum et al., 2016]:

ρ	$\tau_W = 4$	$\tau_W = 8$	$\tau_W = 12$	$\tau_W = 16$
0.100	1.275	1.2967	1.2942	1.2832
0.112	1.313	1.436	1.485	1.4487
0.124	1.408	1.516	1.574	1.5736

Table: Ratios of τ_{exp} for HMC to τ_{exp} with FTHMC at fixed $\delta\tau_G = 1/48$, varied Wilson flow time τ_W.

- Autocorrelation times of Wilson-flowed energies reduced by a factor growing with the smearing parameter ρ — up to ≈ 1.5 at $\rho = 0.124$
- statistics: $\approx$ 190–400 (typically ≈ 230) thermalized configurations per ensemble
- Master-field technique determines the autocorrelation coefficients from a small number of configurations

Longer Trajectory Length Decreases Autocorrelation

Christoph Lehner (2024):

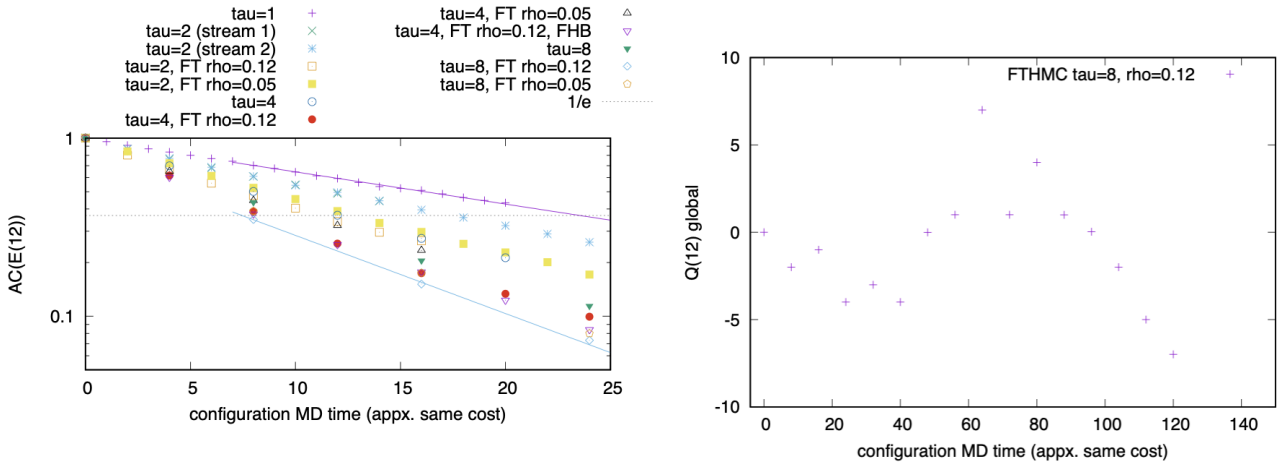

Figure: Autocorrelation of Wilson energy with $\tau_W = 12$ vs. MC time in MD units, measured on $62^3 \times 96$ lattice (left) and topological charge Q vs. MC time, measured on $128^3 \times 288$ lattice (right)

- The effect of longer trajectory length is additive (a factor of ≈ 3.5)
- GPT implementation is used for computation [Lehner et al.,]
- Q is measured on the lattice at the physical point $a^{-1} \approx 3.5$ GeV with $2 + 1f$ DWF

This Work

Two directions, both at matched molecular-dynamics (MD) cost:

- **Kernel scan**: at fixed $\rho = 0.12$
  1. the type of the smearing kernel
  2. the number of its applications
- **Trajectory-length scan**: for HMC and FTHMC with a fixed kernel
  - $\tau_{\mathrm{MD}} = 1, 2, 4$
  - Does the additive gain persist under the field transformation with the new kernel?

Strategy:

- quenched ensembles for fast turnaround
- observables and analysis identical to the previous study
- autocorrelation coefficients again via the master-field technique [Lüscher, 2018, Bruno et al., 2023]

The Kernel

One transformation step is a stout-like smearing update [Morningstar and Peardon, 2004]

$$\mathcal{F} : U_\mu(x) \mapsto e^{\,Q_\mu(x)}\, U_\mu(x), \qquad Q_\mu(x) = -\rho\, \mathcal{P}\Big[U_\mu(x)\, C_\mu(x)^\dagger\Big],$$

with $\mathcal{P}$ the traceless anti-hermitian projection.
The **kernel** is the choice of staple sum $C_\mu(x)$:

p: $$C_\mu^{(p)}(x) = \sum_{\pm\nu\neq\mu} U_\nu(x)\, U_\mu(x+\hat{\nu})\, U_\nu(x+\hat{\mu})^\dagger$$

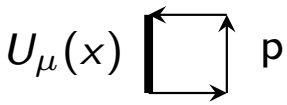

r: $$C_\mu^{(r)}(x) = \sum_{\pm\nu\neq\mu} U_\nu(x)\, U_\nu(x+\hat{\nu})\, U_\mu(x+2\hat{\nu}) \times U_\nu(x+\hat{\mu}+\hat{\nu})^\dagger\, U_\nu(x+\hat{\mu})^\dagger$$

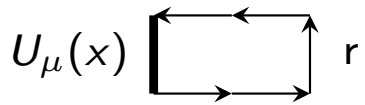

- **p** — 1×1 plaquette staples: the standard stout link [Morningstar and Peardon, 2004]
- **r** — 2×1 rectangle staples, smeared link on the short side

The Masking Scheme

- A single transformation step is composed of **masked sub-steps**
- Each sub-step updates only a subset of links
- The staple of an updated link never contains another updated link
  - $\Rightarrow$ each update is independent
  - $\Rightarrow$ the Jacobian factorizes into per-link blocks

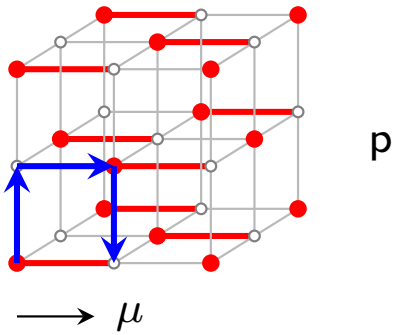

- **p**: red–black *site* checkerboard mask
- **r**: the rectangle staple reaches $U_\mu(x \pm 2\hat{\nu})$ — the *same* site parity
  - a coarser 2×2-*cell* red–black in the plane $\perp \mu$
  - uniform along μ

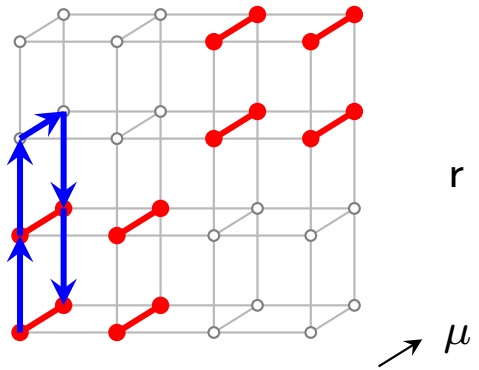

red = updated; blue = example staple

The Kernel: Two-Step Compositions

Beyond a single step, kernels can be **composed** — two full smearing updates in sequence:

$$\mathcal{F}_{k_2 k_1} = \mathcal{F}_{k_2} \circ \mathcal{F}_{k_1} : \quad U' = e^{Q^{(k_1)}[U]}\, U, \qquad U'' = e^{Q^{(k_2)}[U']}\, U'.$$

Note: *not* a single update with a combined staple sum:

$$U'' \neq e^{Q^{(k_1)}[U] + Q^{(k_2)}[U]}\, U.$$

- Each step keeps its own exactly computable Jacobian factor
- The same upper bound $|\rho| < 1/8 = 0.125$ applies to every step (we use $\rho = 0.12$)

The scan: **6 kernels** — single-step **p**, **r** and compositions **pp**, **pr**, **rp**, **rr** — compared against HMC at matched MD cost.

Table of Contents

Run Parameters

Lattice Parameters:

- quenched SU(3) on a lattice of size $24^3 \times 40$
- Iwasaki gauge action at $\beta = 2.9$
- $a^{-1} = 2.81(6)$ GeV (scale set by $m_\rho = 770$ MeV) [Ali Khan et al., 2001]
- $\Rightarrow aL \approx 1.7$ fm

HMC Parameters:

- kernels: p, r, pp, pr, rp, rr at fixed $\rho = 0.12$
- trajectory lengths $\tau_{\mathrm{MD}} = 1, 2, 4$ for HMC and kernel r
- $\tau_{\mathrm{MD}} = 2$ for the rest
- $\therefore$ 11 chains in total
- Metropolis switched on per chain once the plaquette stabilized

Statistics

chain	τ_{MD}	N_{cfg}	N_{therm}	chain	τ_{MD}	N_{cfg}	N_{therm}
HMC	1	609	309	p	2	245	186
HMC	2	604	304	pp	2	132	101
HMC	4	600	300	pr	2	97	81
r	1	155	120	rp	2	97	81
r	2	74	57	rr	2	97	84
r	4	95	82				

Table: Total and thermalized configurations per chain (the FTHMC chains are still growing)

Machine

- Simulation is carried out on Aurora at Argonne National Laboratory
- Master-field analysis is performed on Andes at Oak Ridge National Laboratory

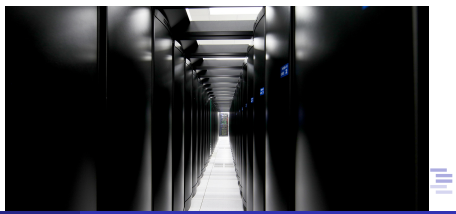

$\langle dH \rangle$

chain	τ_{MD}	s	$\langle dH \rangle$	$\langle e^{-dH} \rangle$	chain	τ_{MD}	s	$\langle dH \rangle$	$\langle e^{-dH} \rangle$
HMC	1	2	0.039(18)	1.013(19)	p	2	4	0.007(8)	1.000(8)
HMC	2	2	0.084(18)	0.965(18)	pp	2	4	0.056(27)	0.980(26)
HMC	4	2	0.048(21)	1.020(23)	pr	2	6	0.005(13)	1.001(13)
r	1	6	0.006(8)	0.998(8)	rp	2	6	0.005(9)	0.999(9)
r	2	6	0.014(10)	0.989(10)	rr	2	6	0.088(26)	0.943(25)
r	4	6	0.004(11)	1.001(11)					

- $\langle e^{-dH} \rangle = 1$ within errors for every chain where $\delta\tau_{\mathrm{MD}} \approx 1/(24\,s)$

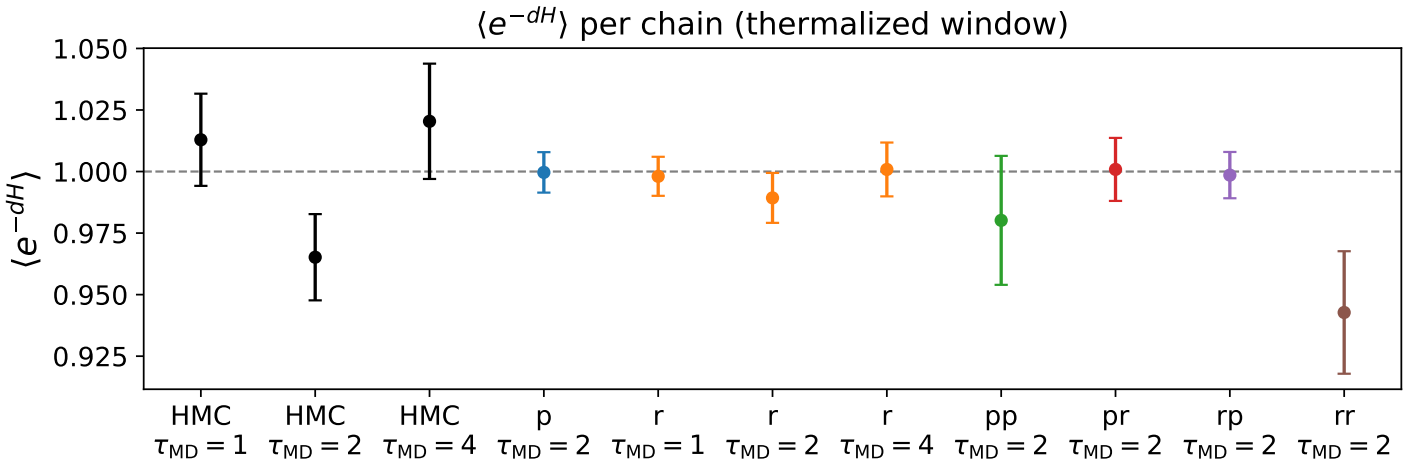

dH Distributions

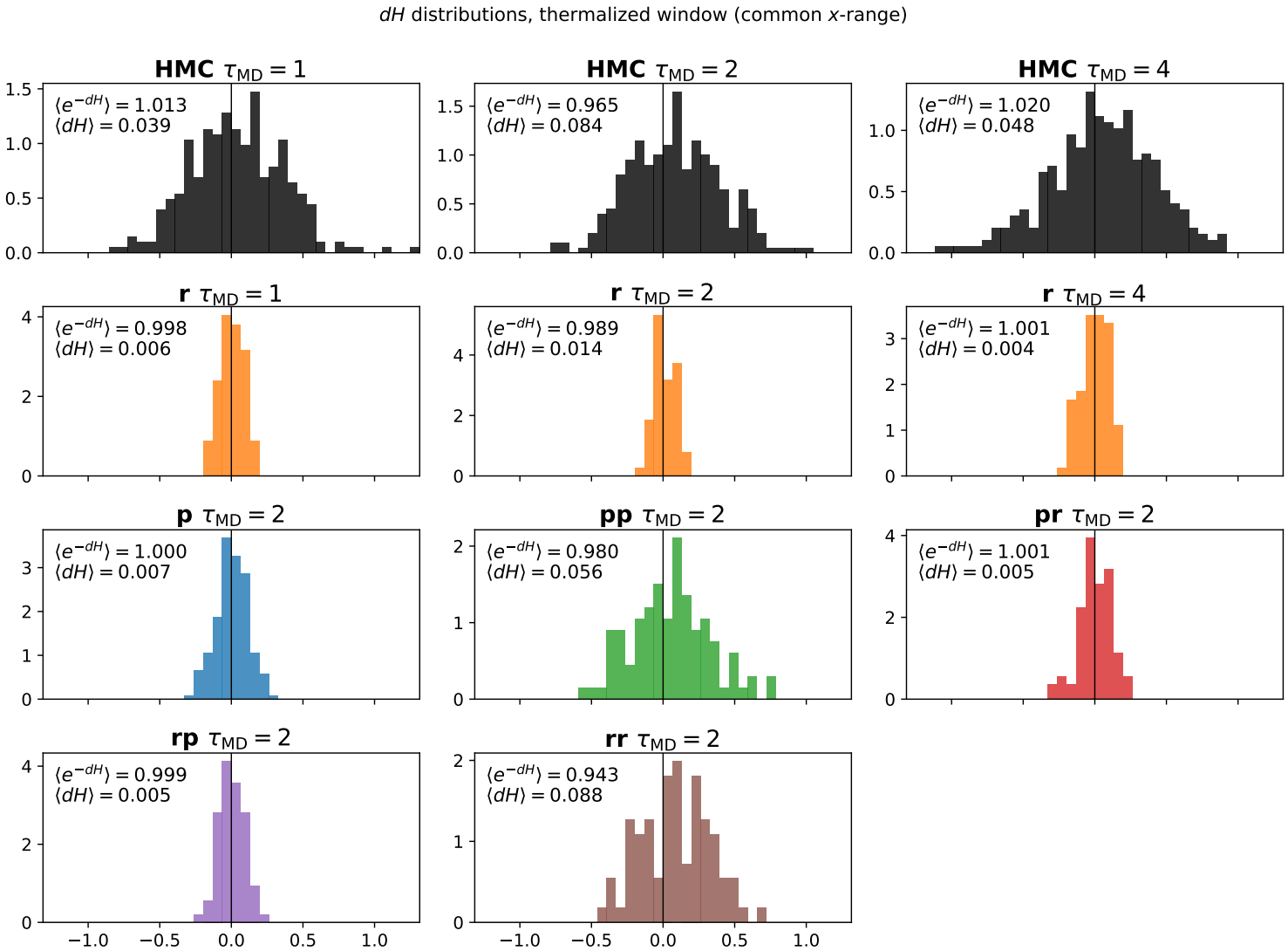

- *dH* fluctuations are widest for HMC and for the pp and rr kernels

Plaquettes

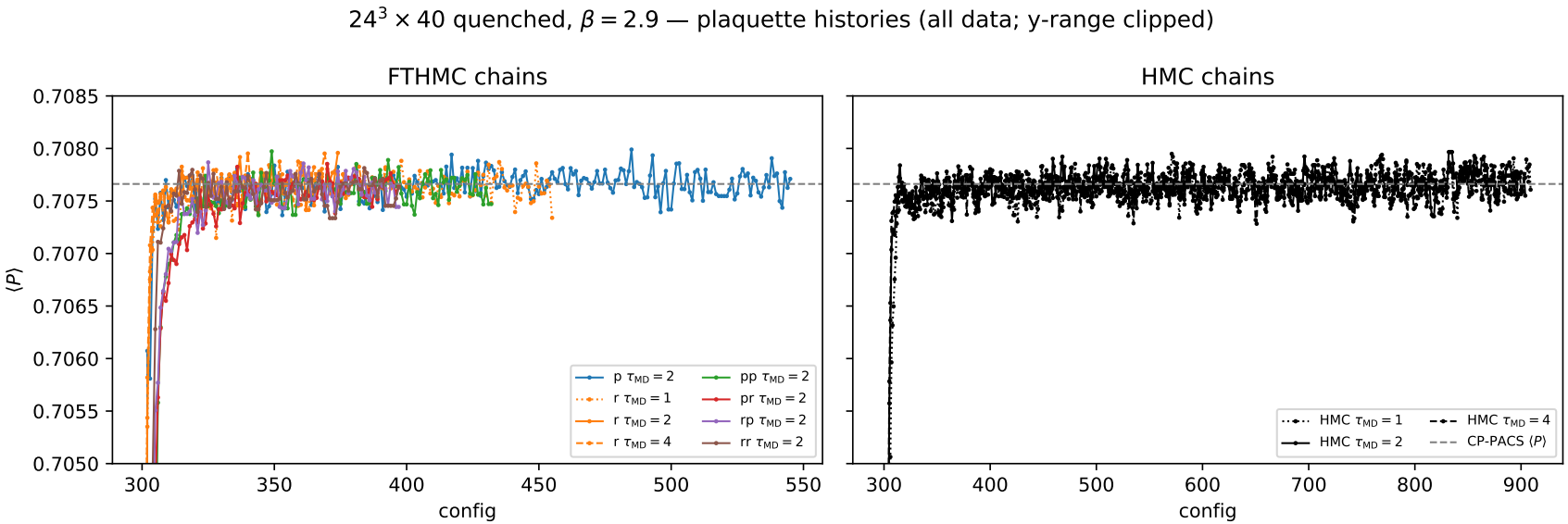

Figure: Plaquette histories, all 11 chains and all configurations

- every chain thermalizes onto and fluctuates around the CP-PACS reference value $\langle P \rangle = 0.707662(5)$ [Ali Khan et al., 2001] (per-chain values: appendix)

Table of Contents

Wilson Flowed Energies

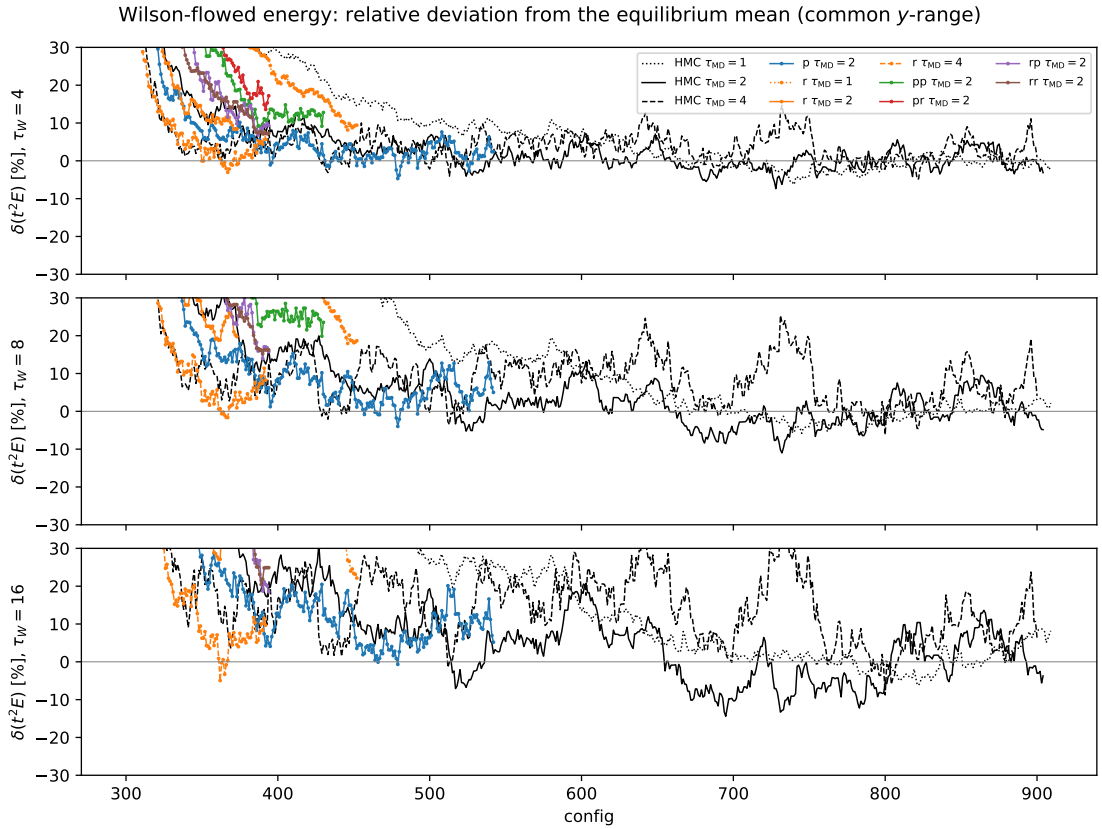

Figure: Relative deviation of the Wilson-flowed energy t^2E from its equilibrium mean, for flow times $\tau_W = 4, 8, 16$ (rows); common y-range.

- larger $\tau_W \Rightarrow$ increasingly infrared: slower, larger fluctuations

Table of Contents

Master-Field Technique

The Problem:

- The standard Autocorrelation Coefficient (ACC) estimator correlates the *volume average* $\langle\langle A \rangle\rangle$ along the chain
- It needs $T \gg \tau_{\mathrm{exp}}$ configurations
- Our FTHMC chains have $\mathcal{O}(50)$

The Idea [Lüscher, 2018]: **Let the volume supply the statistics**

- Compute the ACC of the *local fluctuation* $A'(x) = A(x) - \langle\langle A \rangle\rangle$ at every site x
- Then volume-average the result to get the local ACC:

$$\rho(t) = \langle\langle \Gamma'(t) \rangle\rangle / \langle\langle \Gamma'(0) \rangle\rangle$$

- Each configuration pair contributes V spatially correlated samples
  - $\approx V/\xi^4$ independent ones with ξ the correlation length of the flowed field
- Note: the volume-average (zero-momentum) mode is removed by construction — A' carries only the finite-wavelength fluctuations, the complement of what the standard estimator correlates

Autocorrelation for Local Quantities

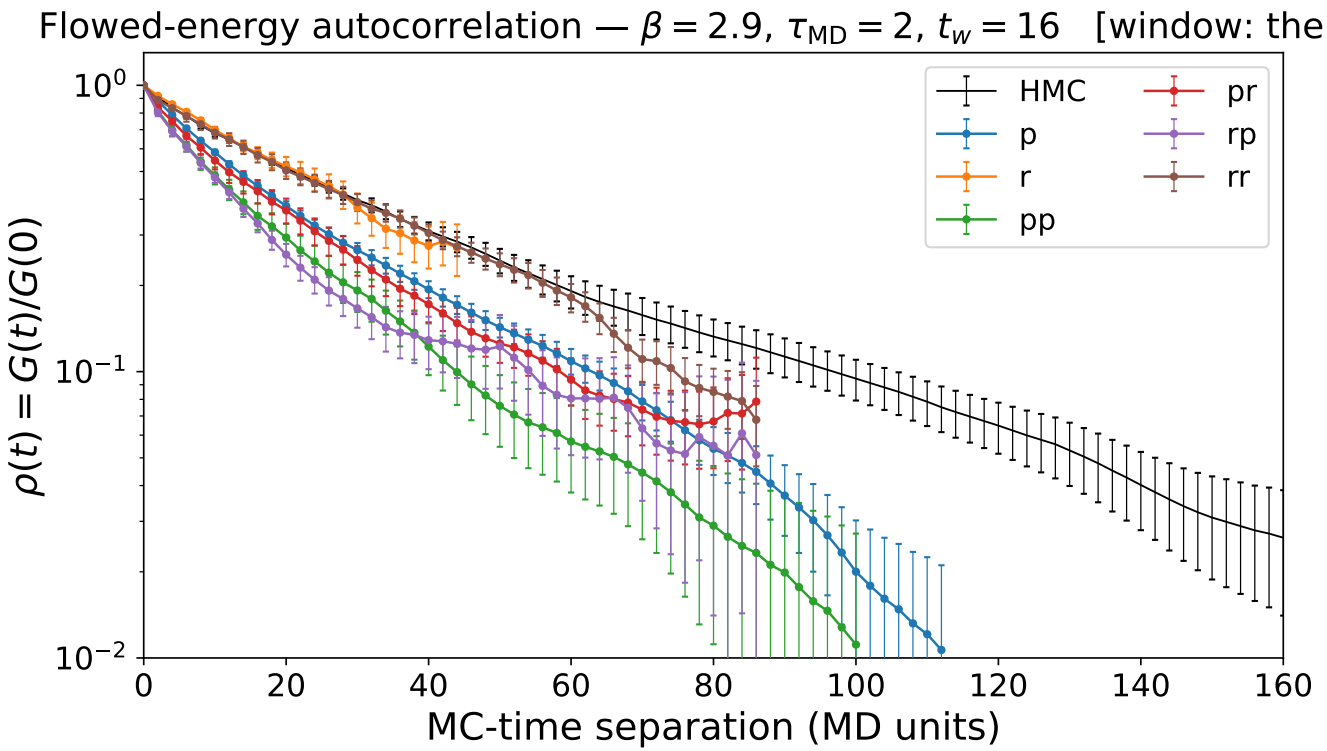

Figure: Flowed-energy ACC at $\tau_{\mathrm{MD}} = 2$, $\tau_W = 16$, thermalized windows; curves cut at the noise floor.

- clear kernel hierarchy in decorrelation speed: rp $>$ pp $\approx$ pr $>$ r $\approx$ p $>$ rr $>$ HMC

Trajectory-Length Dependence

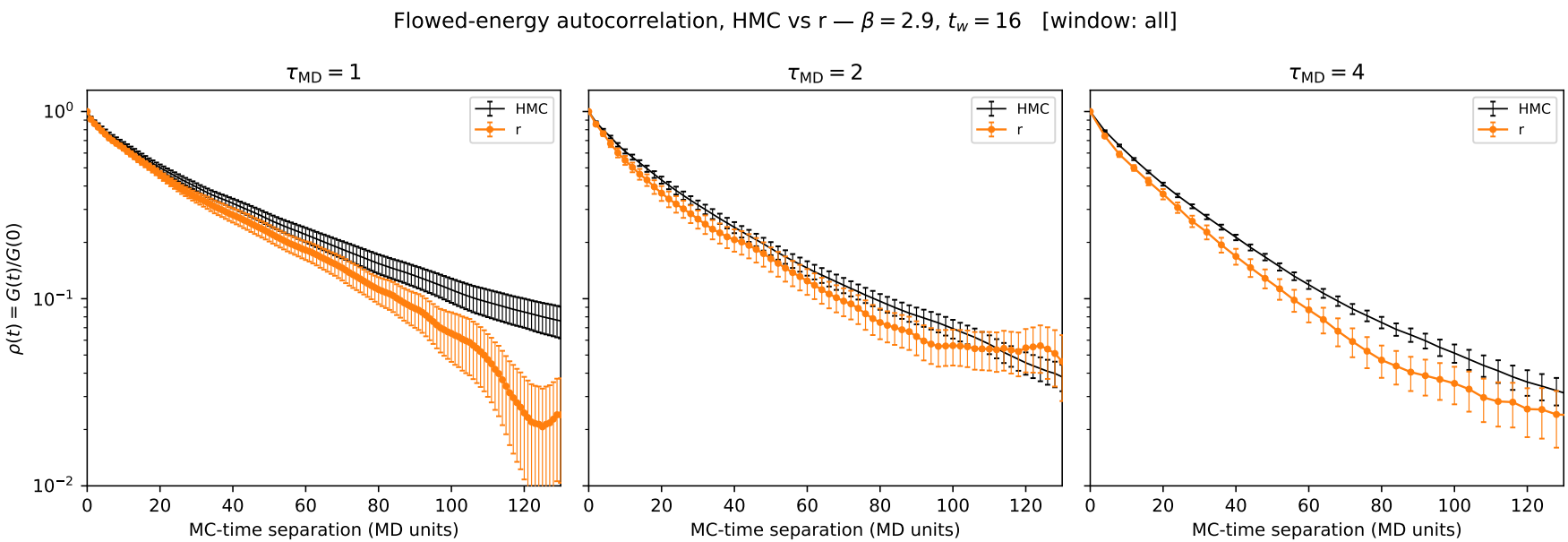

Figure: Flowed-energy ACC with master-field errors, HMC vs. r, one panel per $\tau_{\mathrm{MD}} = 1, 2, 4$; x in MD units ($\tau_W = 16$, window: all).

- the x axis is MD time ($t \times \tau_{\mathrm{MD}}$): equal x = equal MD cost
- even at matched MD cost, longer τ_{MD} decorrelates faster — the additive gain, for HMC and r alike
- r lies at or below HMC in every panel

Autocorrelation Times

$\tau_{\mathrm{exp}}^{\mathrm{MD}}(\mathrm{HMC})/\tau_{\mathrm{exp}}^{\mathrm{MD}}(\mathrm{kernel})$ at matched τ_{MD}, thermalized windows:

kernel	τ_{MD}	$\tau_W = 4$	$\tau_W = 8$	$\tau_W = 12$	$\tau_W = 16$
p	2	1.55	1.59	1.58	1.56
r	2	2.34	1.74	1.58	1.60
r	4	1.51	1.65	1.72	1.78
pp	2	**1.90**	**2.07**	**2.04**	**1.96**
pr	2	1.96	1.91	1.88	1.90
rp	2	**2.12**	**2.22**	**2.27**	**2.45**
rr	2	1.32	1.21	1.22	1.30

Table: Ratio > 1: kernel faster than HMC at matched τ_{MD} (notebook Sec. 9.3).

- pp ≈ 2.0, rp $\lesssim 2.5$ (not yet converged), pr ≈ 1.9; single p ≈ 1.6; r comparable at a higher cost per step; rr the weakest
- r at $\tau_{\mathrm{MD}} = 1$ omitted: its HMC baseline has no measurable τ ($T \approx 3.6\,\tau_{\mathrm{int}}$, topology frozen)

Is the Factor of 2 Real at Matched Cost?

Why τ_{exp} in MD units is the cost metric:

- for ensemble generation with dynamical fermions:
  - the computation of the **fermion force dominates** the cost per MD unit
  - its cost is kernel-independent
- FT overhead:
  - ε per smearing step per MD step
  - 2ε for two-step kernels
  - $\Rightarrow$ marginal
- acceptance 0.86–0.97 across all chains
  - HMC baselines 0.86–0.88

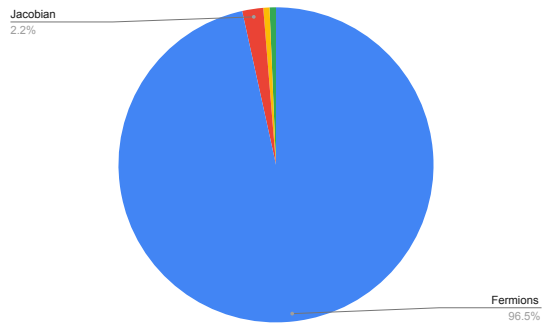

Figure: FTHMC cost breakdown ($2+1$ DWF, thermalized config.): fermions 96.5%, Jacobian 2.2%.

- $m_\pi = 371(5)$ MeV [Blum et al., 2016]
- quenched wall-clock times are *not* the cost metric
- with dynamical fermions the gauge force is a negligible fraction of the cost
- the quenched runs only rank the kernels

Table of Contents

Summary and Outlook

- The FTHMC kernel matters:
  - At fixed ρ and matched MD cost, two-step compositions (rp, pp) reduce τ_{exp} of Wilson-flowed energy by a factor of $\approx$ 2–2.5 over HMC (thermalized windows; rp not yet converged — upper bound)
- Rectangle-based kernels show no advantage over the plaquette kernel: r matches p's gain only at a higher cost per step; rr trails
- At a fixed number of smearing steps, the cheaper plaquette-based kernels perform better
- Master-Field technique again allows us to measure autocorrelation coefficients from a small number of configurations (57–186 per FTHMC chain)
- TODO: Finalize rectangle-kernel statistics and topological-charge ACC
- TODO: Kernel tuning (ρ per kernel, deeper compositions), dynamical fermions, finer lattices

Thank you!


Ali Khan, A. et al. (2001).
Kaon B parameter from quenched domain-wall QCD.
Phys. Rev. D, 64:114506.


Blum, T. et al. (2016).
Domain wall QCD with physical quark masses.
Phys. Rev. D, 93(7):074505.


Bruno, M., Cè, M., Francis, A., Fritzsch, P., Green, J. R., Hansen, M. T., and Rago, A. (2023).
Exploiting stochastic locality in lattice QCD: hadronic observables and their uncertainties.
JHEP, 11:167.


Lehner, C., Bruno, M., Richtmann, D., Schlemmer, M., Lehner, R., Knüttel, D., Wurm, T., Jin, L., Bürger, S., Hackl, A., and Klein, A.
Grid Python Toolkit (GPT).


Lüscher, M. (2010).

Autocorrelation

Notation

- Observable: $A(x)$
- Measurement: $a_i(x)$
- Volume Average: $\langle\langle A \rangle\rangle = (1/V) \sum_x A(x)$
- Ensemble Average: $a = \langle a_i(x) \rangle = \langle \langle\langle A \rangle\rangle \rangle$
- Autocovariance: $\Gamma^V(t) = \langle \langle\langle a_i \rangle\rangle \langle\langle a_{i+t} \rangle\rangle \rangle$
- Autocorrelation Coefficients (ACC): $\rho^V(t) = \Gamma^V(t)/\Gamma^V(0)$

Estimators:

- $\langle a(x) \rangle \to \bar{a}(x) = \frac{1}{T} \sum_{i=1}^{T} a_i(x)$
- T: length of Markov chain approximating the ensemble

Master-Field Technique: the Idea

The Problem:

- The standard ACC estimator correlates the *volume average* $\langle\langle A \rangle\rangle$ along the chain — it needs $T \gg \tau_{\mathrm{exp}}$ configurations; our FTHMC chains have $\mathcal{O}(50)$

The Idea [Lüscher, 2018]: **Let the volume supply the statistics**

- Correlate the *local fluctuation* $A'(x) = A(x) - \langle\langle A \rangle\rangle$ along the chain, at every site x; then volume-average the result:

$$\rho(t) = \langle\langle \Gamma'(t) \rangle\rangle / \langle\langle \Gamma'(0) \rangle\rangle$$

- Each configuration pair contributes V correlated samples $\approx V/\xi^4$ independent ones, with ξ the correlation length of the flowed field
- Note: This is the ACC of the *local* fluctuations (the volume-average mode is subtracted)

Master-Field Error Estimate: the Idea

- These V samples are *not* independent: sites are correlated over the observable's correlation length ξ
- So the error of $\rho(t)$, σ_ρ, is built from the position-space covariance of the local correlators, summed over separations $|y| \leq R$
  - typically the lattice is grouped into blocks of size l_B to reduce the computational cost [Bruno et al., 2023]
- Approximation: Grow R until σ_ρ **saturates** (R_{sat})
  - The volume admits at most $R = L/2 = 12$ (periodic wrap)
- checked per chain and per flow time

Error via Master-Field Approach

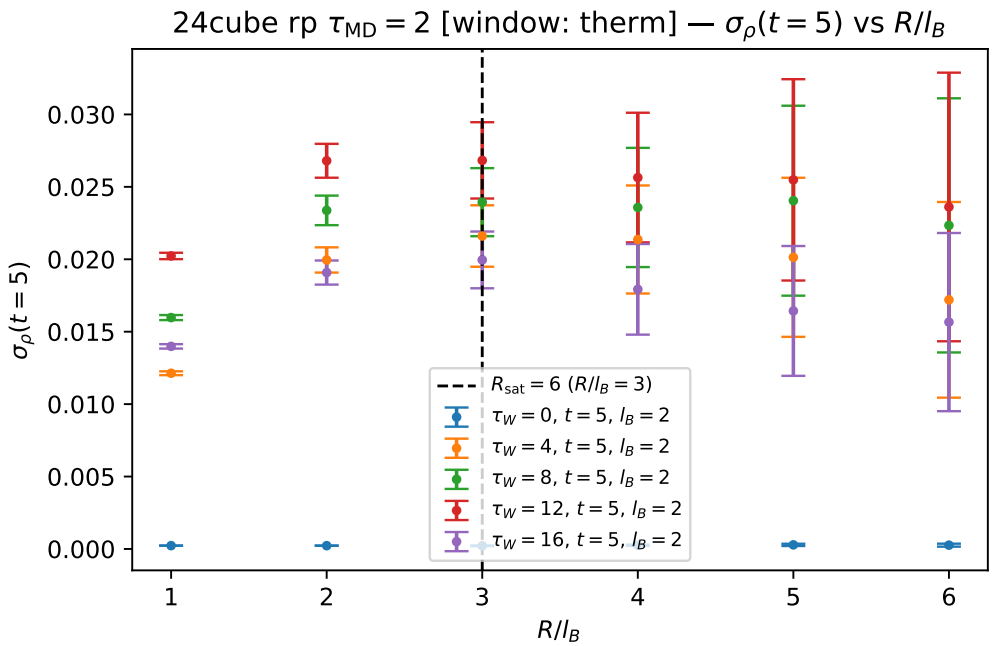

Figure: $\sigma_\rho(t = 5)$ vs. summation radius R/l_B per flow time (rp, $\tau_{\mathrm{MD}} = 2$, window: therm; checked per chain). Dashed line: per-chain R_{sat}.

- R_{sat} is a bias–variance trade-off: too small biases σ_ρ low; too large makes σ_ρ itself noisy
- all 11 chains checked: the drift beyond the per-chain R_{sat} stays within $\sigma_\rho(R)$'s own uncertainty

Per-Chain τ_{exp} Fits

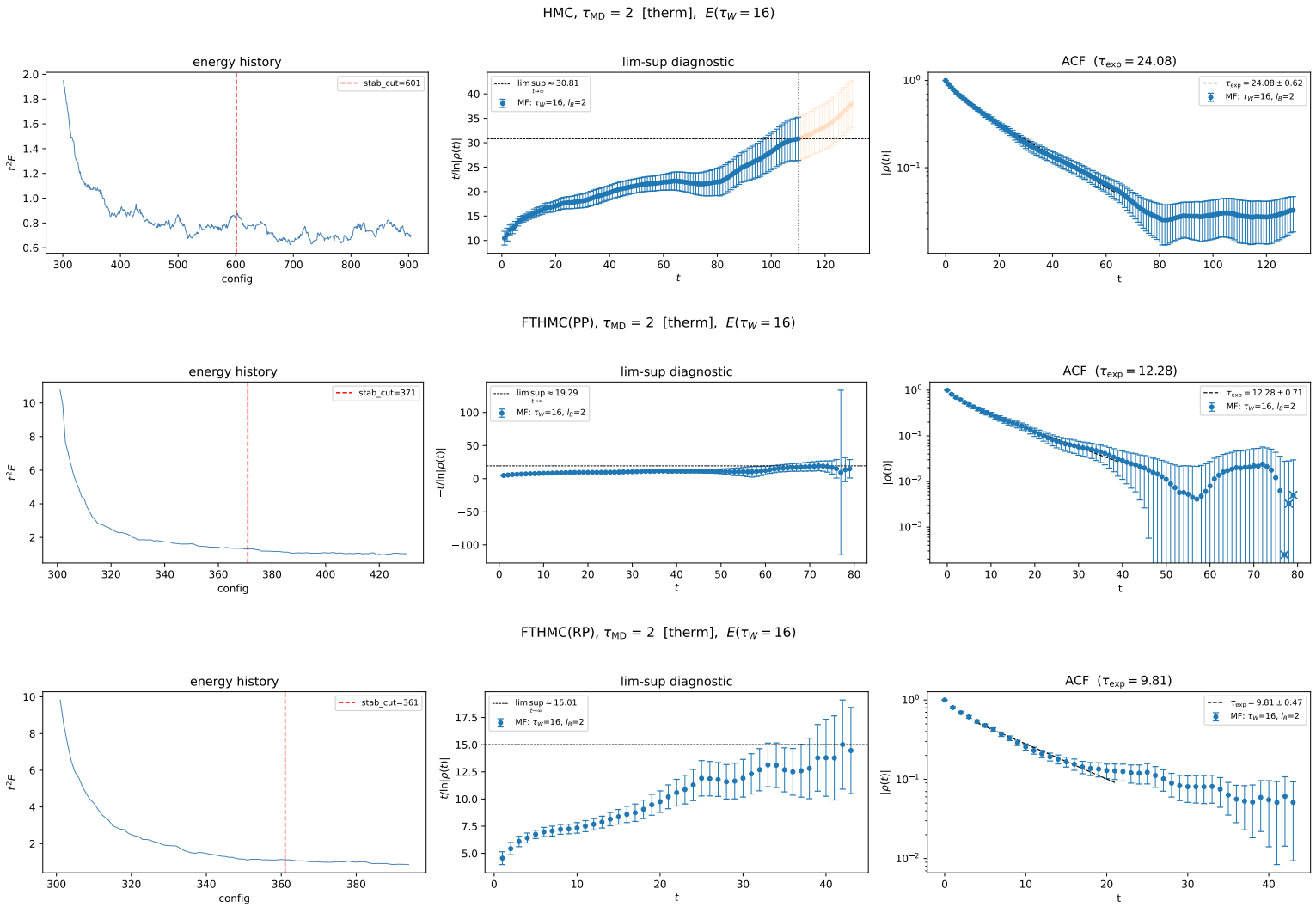

- lim-sup panels and exponential fits per chain ($\tau_W = 16$, window: therm); fit windows set per window/chain

Autocorrelation for Local Quantities (window: all)

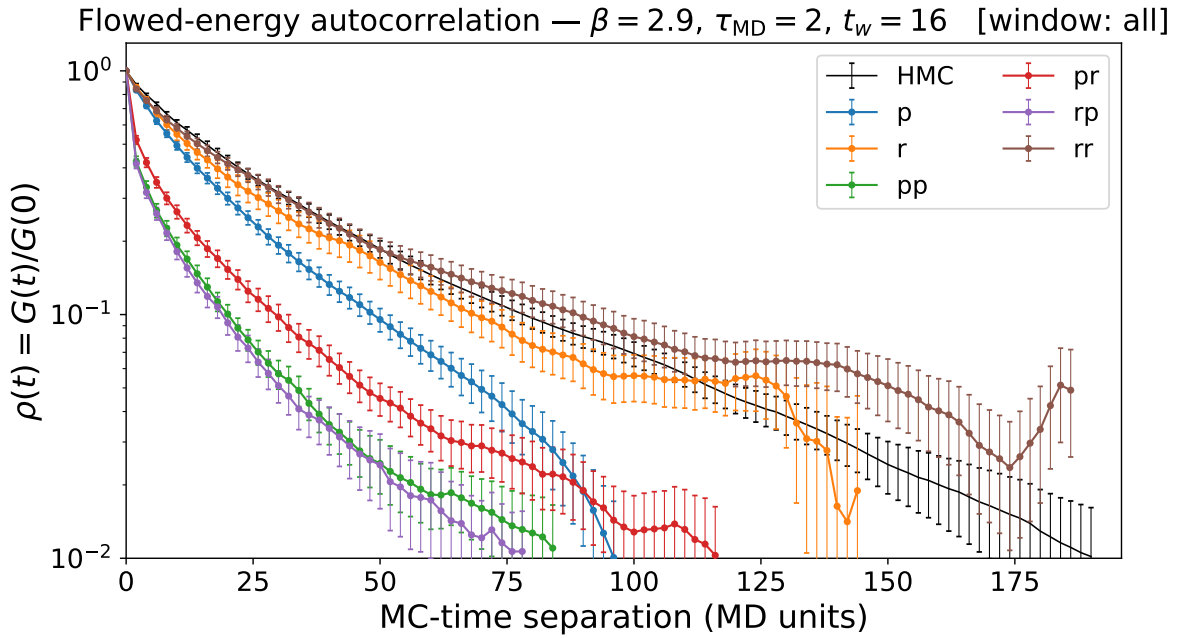

Figure: As the main-deck figure, but over all configs > 300 — includes the pre-thermalization (forced-accept) segment.

- rp fastest in both windows; the r family and rr shift the most between windows — transient contamination

Autocorrelation Times (window: all)

$\tau_{\mathrm{exp}}^{\mathrm{MD}}(\mathrm{HMC})/\tau_{\mathrm{exp}}^{\mathrm{MD}}(\mathrm{kernel})$ at matched τ_{MD}, window: all

kernel	τ_{MD}	$\tau_W = 4$	$\tau_W = 8$	$\tau_W = 12$	$\tau_W = 16$
p	2	1.56	1.67	1.72	1.76
r†	1	0.97	1.04	1.07	1.09
r	2	1.49	1.38	1.32	1.28
r	4	1.05	1.10	1.20	1.35
pp	2	1.36	1.48	1.60	1.56
pr	2	1.96	1.81	1.66	1.52
rp	2	1.96	2.03	1.97	1.87
rr	2	1.11	1.06	1.02	1.01

Table: Same fit protocol as the headline (therm) table. The window includes the pre-equilibration segment, whose transient bias is kernel-dependent. †: chain $< 5\tau_{\mathrm{int}}$.

τ_{exp} in MD Units (window: all)

kernel	τ_{MD}	$\tau_W = 0$	$\tau_W = 4$	$\tau_W = 8$	$\tau_W = 12$	$\tau_W = 16$
hmc‡	1	1.12	31.04	38.12	42.68	45.74
hmc	2	$\sim$3.53	37.24	41.31	44.14	46.19
hmc	4	$\sim$6.95	54.59	58.47	61.20	62.96
p	2	$\sim$64.62	23.84	24.68	25.71	26.29
r†	1	$\sim$23.97	31.96	36.71	39.78	42.11
r	2	$\sim$21.76	24.97	29.94	33.35	36.03
r	4	$\sim$52.99	51.79	53.10	51.10	46.60
pp	2	$\sim$42.94	27.41	27.96	27.63	29.53
pr	2	$\sim$27.78	18.98	22.81	26.63	30.42
rp	2	$\sim$28.58	18.98	20.30	22.45	24.76
rr	2	$\sim$28.16	33.53	39.05	43.17	45.63

Table: $\tau_{\mathrm{exp}} \times \tau_{\mathrm{MD}}$ from the master-field fits (notebook Sec. 9.2, window: all). $\sim$: a lim-sup-only estimate enters. $\dagger$: chain $< 5\tau_{\mathrm{int}}$. $\ddagger$: transient-dominated — the therm-window τ_{int} bound (> 85) far exceeds this value.

Error via Master-Field Approach (window: all)

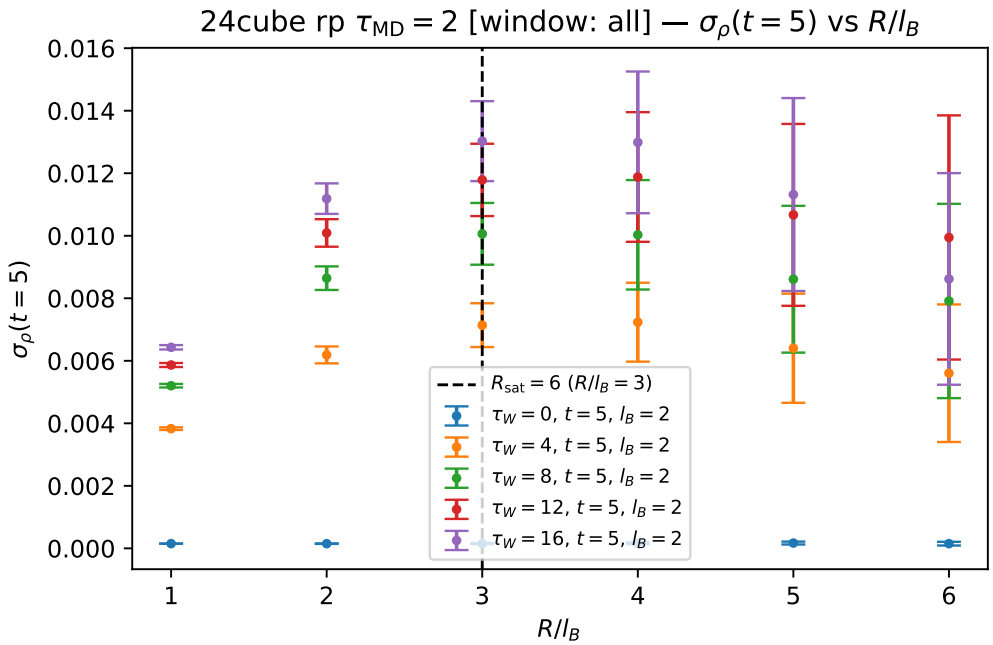

Figure: $\sigma_\rho(t = 5)$ vs. summation radius R/l_B per flow time (rp, $\tau_{\mathrm{MD}} = 2$, window: all). Dashed line: per-chain R_{sat}.

- in the all window, pp/pr show a monotone $\sigma_\rho(R)$ rise toward $L/2$ that is absent in the therm window — tied to the early transient / large-$|Q|$ segment, not equilibrium correlations

Per-Chain τ_{exp} Fits (window: all)

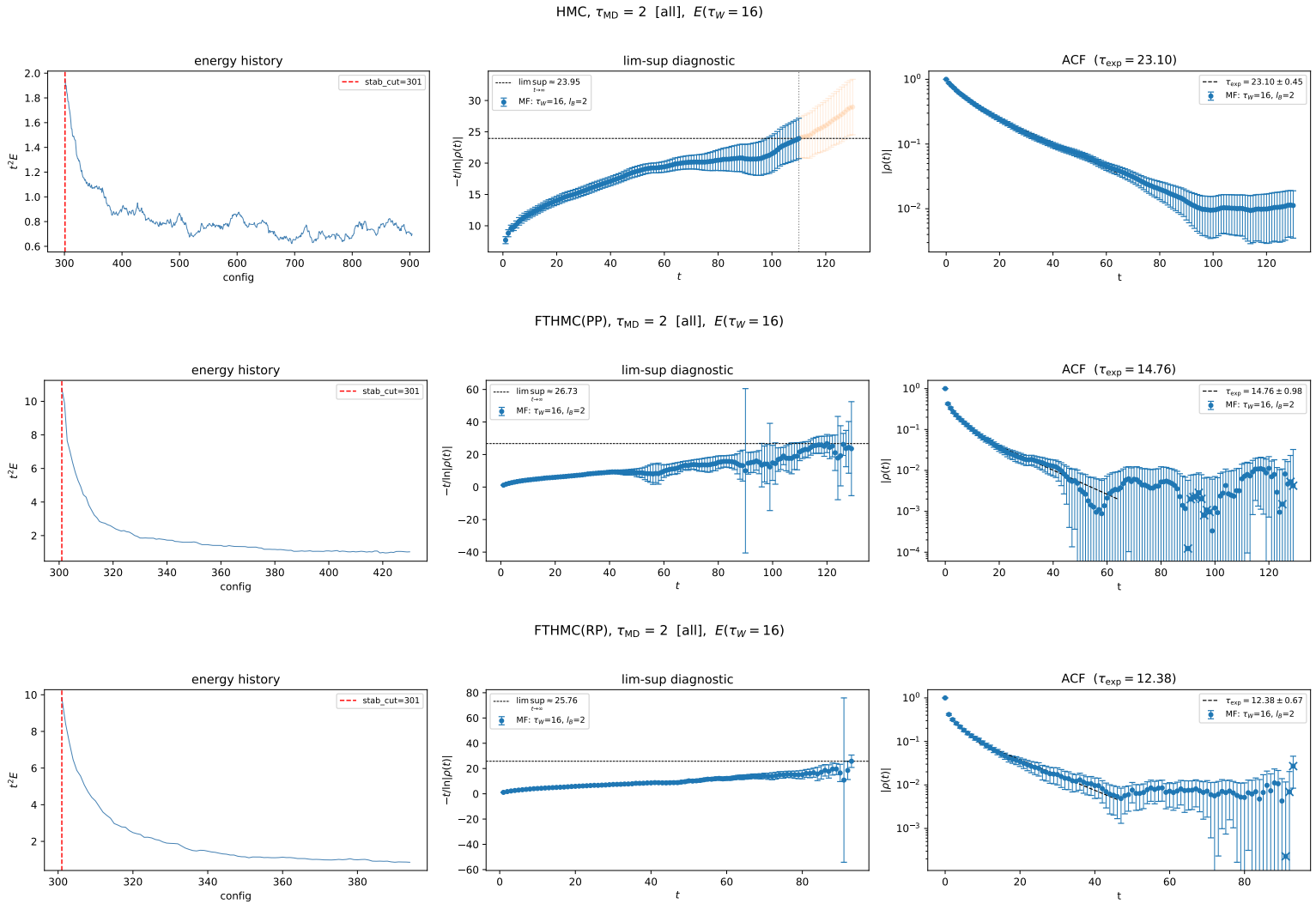

- lim-sup panels and exponential fits per chain ($\tau_W = 16$, window: all)

Acceptance Rates

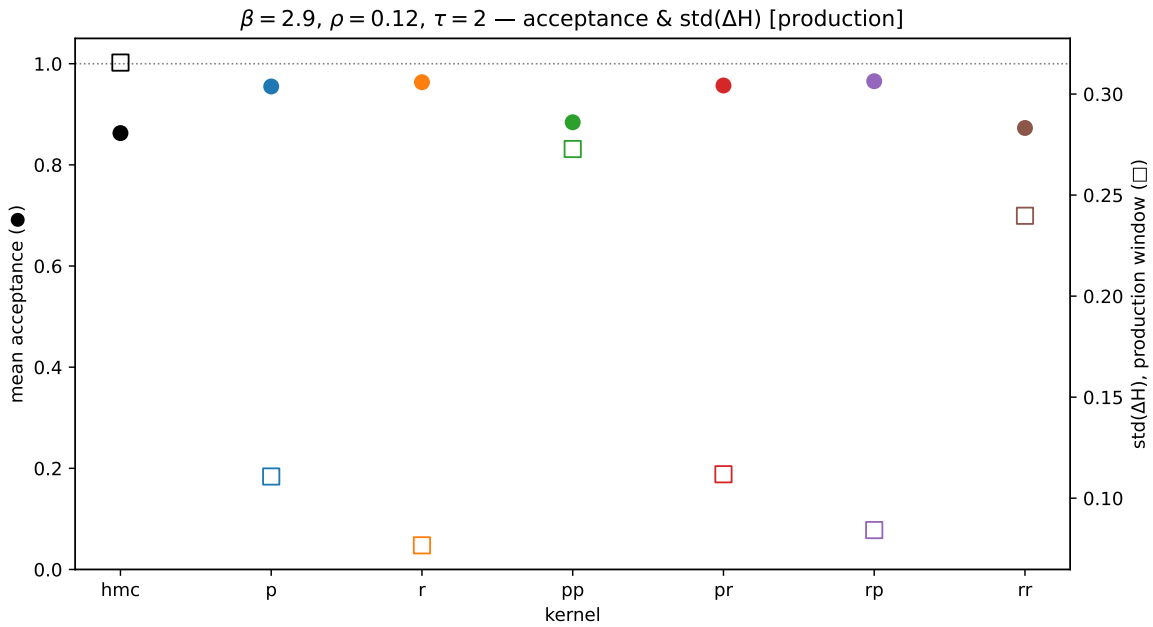

Figure: Acceptance per kernel for the $\tau_{\mathrm{MD}} = 2$ chains.

Trajectory-Length Scan vs. Flow Time

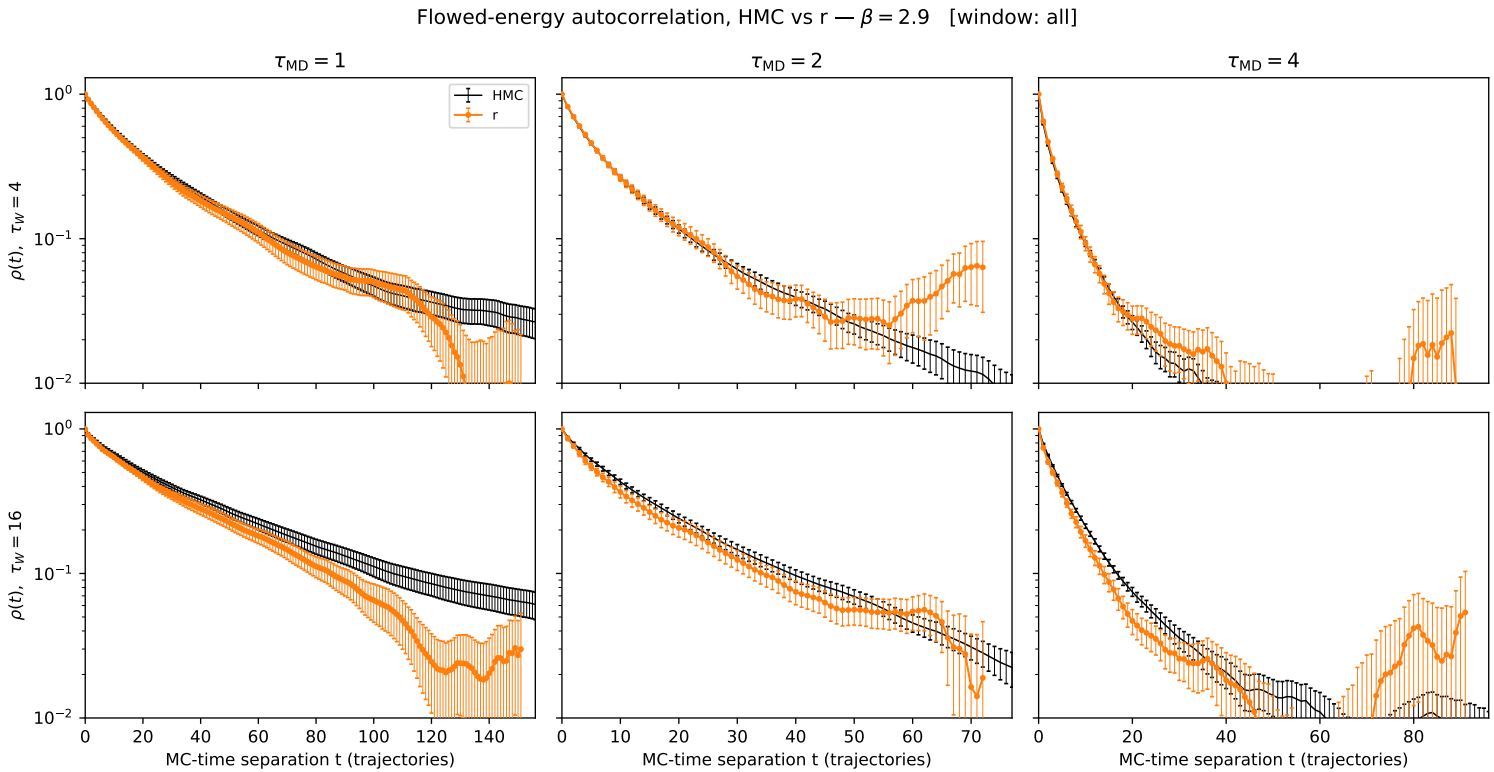

Figure: HMC vs. r per τ_{MD} (columns) at $\tau_W = 4$ and 16 (rows), window: all.

- the r-vs-HMC separation grows from $\tau_W = 4$ to 16 at every trajectory length

Trajectory-Length Scan in MD Units

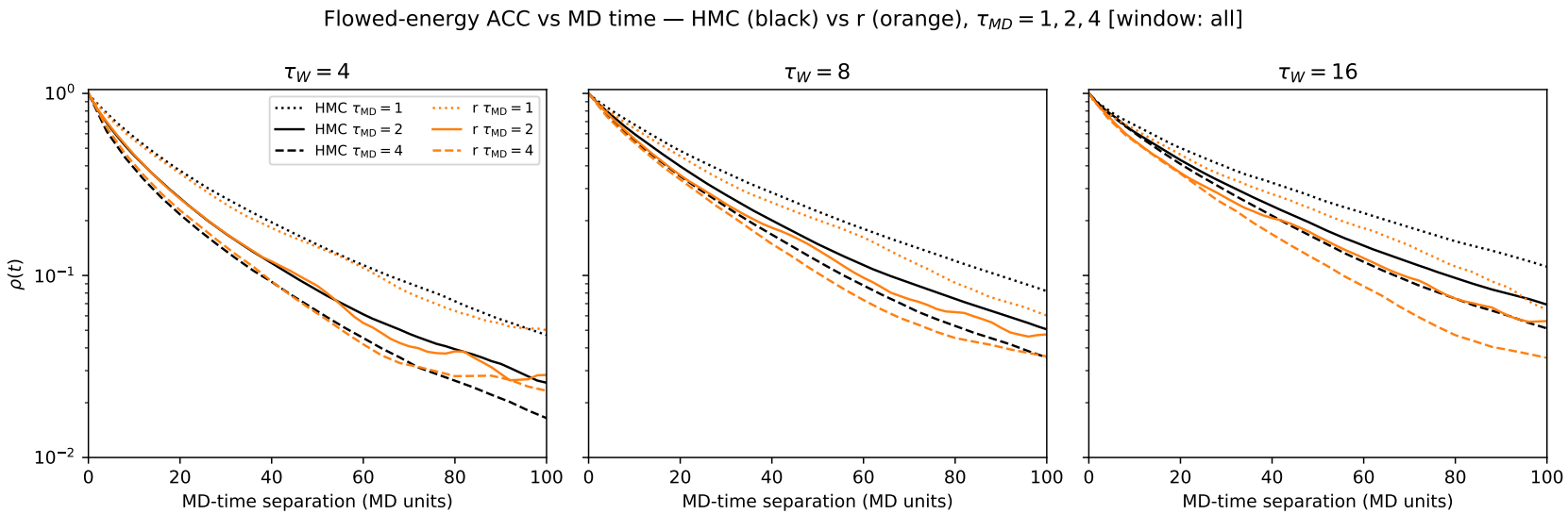

Figure: Flowed-energy ACC vs. MD time, HMC (black) vs. r (orange) at $\tau_{\mathrm{MD}} = 1, 2, 4$, per flow time $\tau_W = 4, 8, 16$ (window: all).

- longer trajectories decorrelate faster even *per MD unit*; the r-vs-HMC gap widens with flow time

Topological-Charge Histories

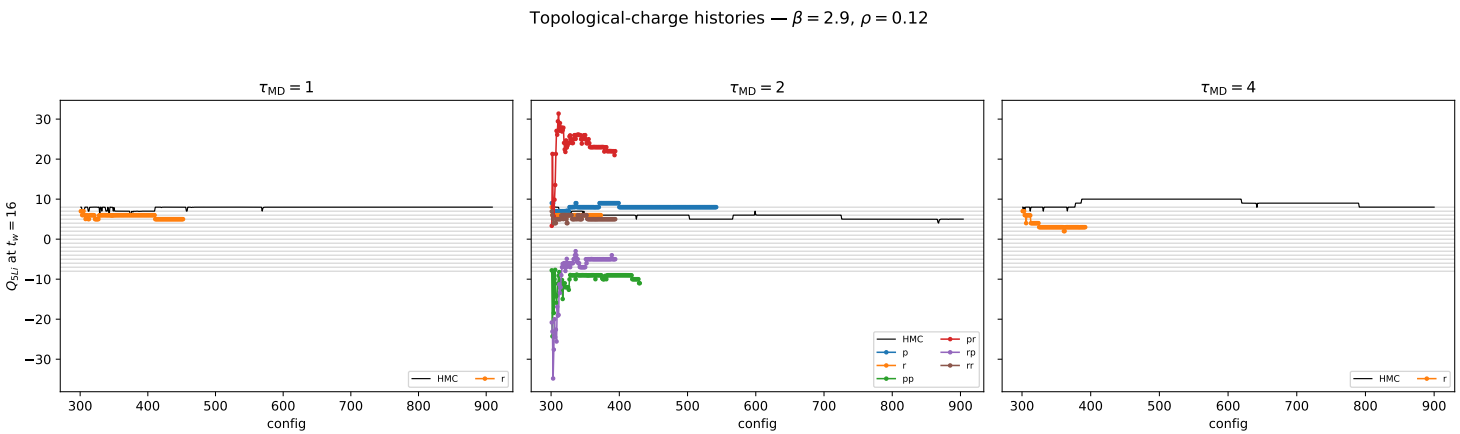

Figure: $Q_{5\mathrm{Li}}$ at $\tau_W = 16$ per chain ($\tau_{\mathrm{MD}} = 1, 2, 4$ panels).

- HMC $\tau_{\mathrm{MD}} = 1$: topology frozen (Q pinned at 8) — excluded from cross-chain references

Relaxation of Wilson Flowed Energy

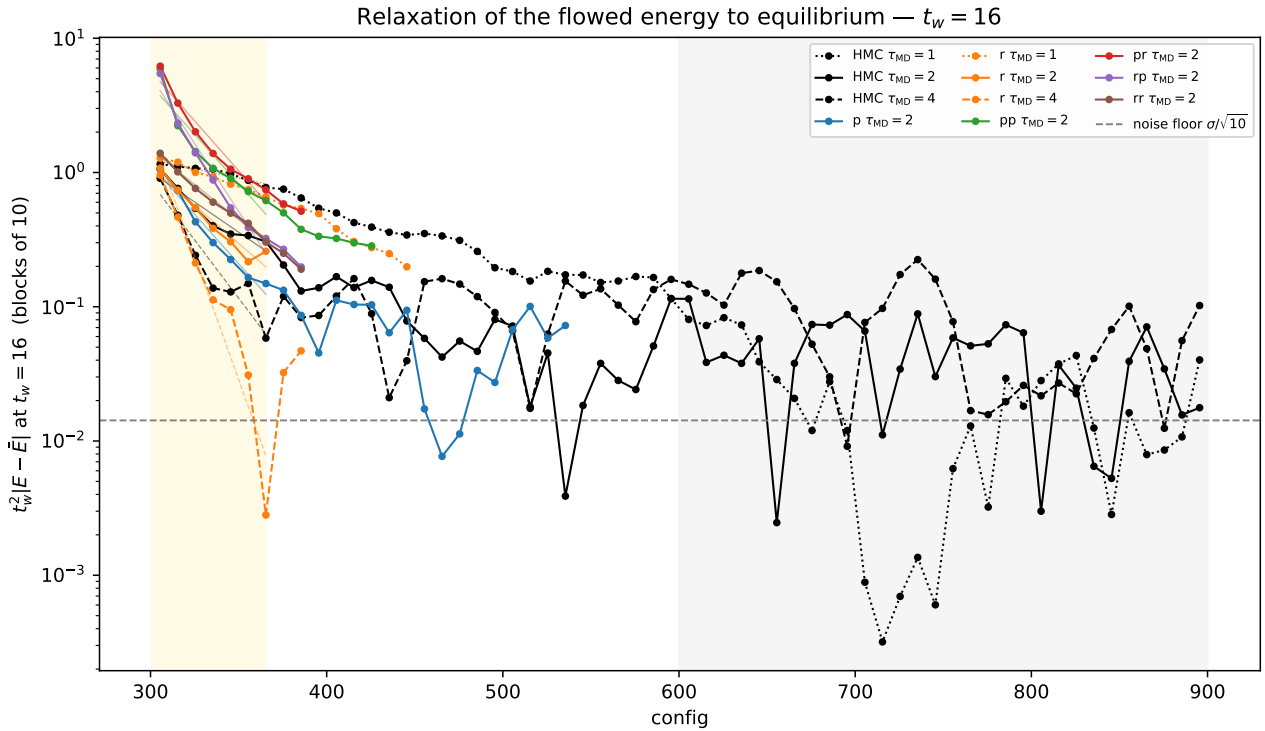

Figure: $\tau_W^2|E - \bar{E}|$ vs. configuration at $\tau_W = 16$ (blocks of 10); shaded band = common fit window.

- "poor man's" thermalization-rate estimate: kernel ordering already visible during relaxation — two-step kernels reach the noise floor fastest, HMC $\tau_{\mathrm{MD}} = 1$ slowest

Master-Field Technique (derivation)

- Instead of ACC of the volume average $\langle\langle A \rangle\rangle = (1/V)\sum_x A(x)$, consider ACC of local observable $A(x)$
- Subtract the volume average: $A'(x) = A(x) - \langle\langle A \rangle\rangle$
- Due to translational invariance, $\mu = \langle A'(x) \rangle = a - a = 0$
- Denote autocovariance of $A'(x)$ at x as $\Gamma'_x(t)$
- Then,

$$\begin{aligned}\Gamma'_x(t) &= \langle (a'_i(x) - \mu)(a'_{i+t}(x) - \mu) \rangle \\ &= \langle a'_i(x) a'_{i+t}(x) \rangle \\ &= \langle (a_i(x) - \langle\langle a_i \rangle\rangle)(a_{i+t}(x) - \langle\langle a_{i+t} \rangle\rangle) \rangle \equiv \langle \mathcal{O}^i_t(x) \rangle\end{aligned}$$

- Approximate $\Gamma'_x(t)$ by $\langle\langle \Gamma'(t) \rangle\rangle$ [Lüscher, 2018]
- Also, $\mathcal{O}^i_t(x) \to \bar{\mathcal{O}}_t(x) \equiv \frac{1}{T-t}\sum_{i=1}^{T-t} \mathcal{O}^i_t(x)$
- Finally, $\rho(t) = \langle\langle \Gamma'(t) \rangle\rangle / \langle\langle \Gamma'(0) \rangle\rangle$

Error via Master-Field Approach (derivation)

- Need:
  $\mathrm{Cov}[\langle\langle\bar{\mathcal{O}}_s\rangle\rangle, \langle\langle\bar{\mathcal{O}}_t\rangle\rangle] \equiv \langle[\langle\langle\bar{\mathcal{O}}_s\rangle\rangle - \langle\mathcal{O}_s\rangle][\langle\langle\bar{\mathcal{O}}_t\rangle\rangle - \langle\mathcal{O}_t\rangle]\rangle = \frac{1}{V}\sum_y C_{st}(y)$
  [Bruno et al., 2023]
- Approximate $C_{st}(y)$ by

$$\langle\langle\mathcal{C}_{st}(y)\rangle\rangle = \frac{1}{V}\sum_x \delta\bar{\mathcal{O}}_s(x+y)\delta\bar{\mathcal{O}}_t(x),\ \delta\bar{\mathcal{O}}_t(x) \equiv \bar{\mathcal{O}}_t(x) - \langle\langle\bar{\mathcal{O}}_t\rangle\rangle$$

- Define $C_{st}(|y| \le R) \equiv \sum_{|y|\le R} C_{st}(y)$
- Determine the value of R s.t. $C_{st}(|y| \le R)$ saturates; truncate the sum beyond R_{sat}; blocks of size l_B
- Here: $R = 12 = L/2$ (periodic-wrap limit), $l_B = 2$

Chain Status

kernel	ρ	τ_{MD}	N_{cfg}	$\langle P \rangle_{\mathrm{all}}$	N_{th}	$\langle P \rangle_{\mathrm{th}}$	cut
hmc	—	1	609	0.707535	309	0.707673	600
hmc	—	2	604	0.707573	304	0.707663	600
hmc	—	4	600	0.707556	300	0.707640	600
p	0.12	2	245	0.707528	186	0.707665	359
r	0.12	1	155	0.707540	120	0.707622	335
r	0.12	2	74	0.707503	57	0.707649	317
r	0.12	4	95	0.707577	82	0.707686	313
pp	0.12	2	132	0.705760	101	0.707610	331
pr	0.12	2	97	0.705941	81	0.707560	316
rp	0.12	2	97	0.706408	81	0.707591	316
rr	0.12	2	97	0.706991	84	0.707591	313

Table: Per-chain status (notebook Sec. 6, 2026-07-30): total and thermalized ($>$cut) config counts, plaquette per window; reference $\langle P \rangle = 0.707662(5)$.

τ_{exp} in MD Units

kernel	τ_{MD}	$\tau_W = 0$	$\tau_W = 4$	$\tau_W = 8$	$\tau_W = 12$	$\tau_W = 16$
hmc‡	1	1.19	36.71	55.85	70.16	80.28
hmc	2	$\sim$3.86	38.70	44.38	46.51	48.16
hmc	4	$\sim$7.47	52.96	59.09	62.61	64.76
p	2	$\sim$57.75	24.98	27.89	29.37	30.88
r†	1	$\sim$17.41	28.35	33.84	37.21	39.37
r†	2	$\sim$7.04	16.51	25.44	29.38	30.11
r†	4	$\sim$22.14	35.02	35.90	36.49	36.44
pp	2	$\sim$25.90	20.40	21.47	22.83	24.56
pr†	2	$\sim$12.35	19.73	23.22	24.75	25.28
rp†	2	$\sim$14.70	18.26	20.02	20.44	19.62
rr†	2	$\sim$12.99	29.24	36.68	38.21	36.95

Table: $\tau_{\mathrm{exp}} \times \tau_{\mathrm{MD}}$ from the master-field fits (notebook Sec. 9.3, window: therm). $\sim$: a lim-sup-only estimate enters. $\dagger$: chain shorter than $5\tau_{\mathrm{int}}$ — the fit cannot see slower modes; likely an underestimate. $\ddagger$: unmeasurable — the τ_{int} lower bound (> 85) exceeds the fitted τ_{exp}; equilibration unresolved within the chain.

Relaxation at $\tau_W = 0$

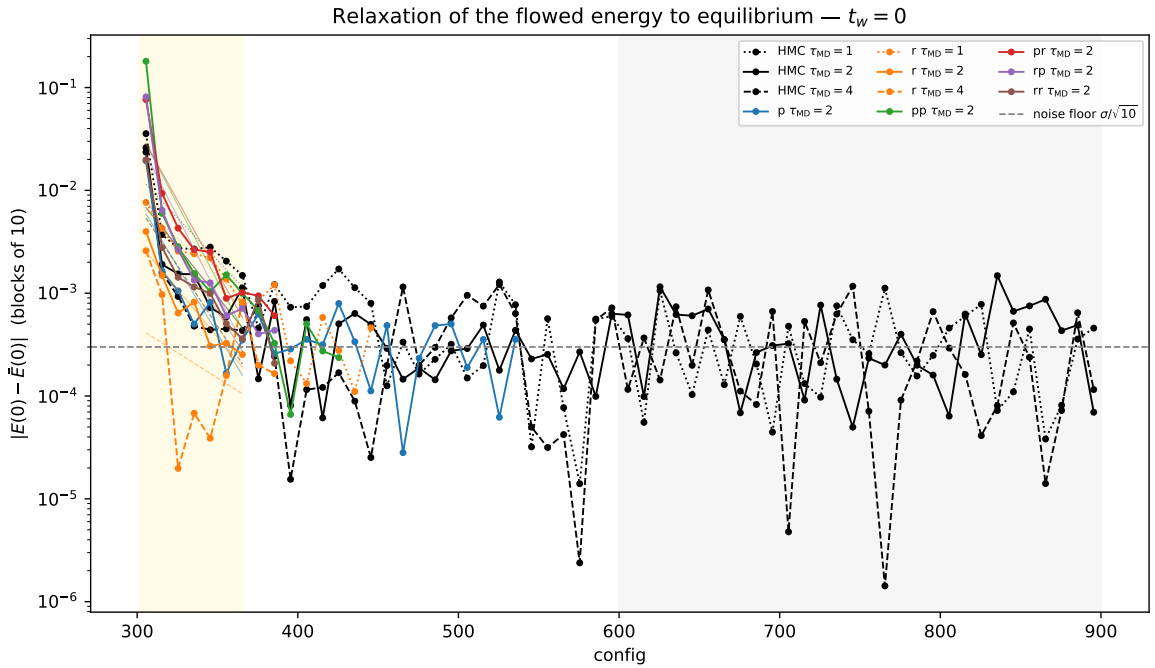

Figure: Unflowed energy relaxes quickly for all chains.

- kernel differences appear only in infrared (large-τ_W) observables